THE STABILITY OF COMPRESSIBLE MIXING LAYERS IN BINARY GASES

F. Kozusko, D.G. Lasseigne
Department of Mathematics and Statistics
Old Dominion University
Norfolk, VA 23529

C.E. Grosch
Department of Oceanography and
Department of Computer Science
Old Dominion University
Norfolk, VA 23529

T.L. Jackson
Institute for Computer Applications in Science and Engineering
NASA Langley Research Center
Hampton, VA 23681-0001

ABSTRACT

We present the results of a study of the inviscid two-dimensional spatial stability of a parallel compressible mixing layer in a binary gas. The parameters of this study are the Mach number of the fast stream, the ratio of the velocity of the slow stream to that of the fast stream, the ratio of the temperatures, the composition of the gas in the slow stream and in the fast stream, and the frequency of the disturbance wave. The ratio of the molecular weight of the slow stream to that of the fast stream is found to be an important quantity and is used as an independent variable in presenting the stability characteristics of the flow. It is shown that differing molecular weights have a significant effect on the neutral-mode phase speeds, the phase speeds of the unstable modes, the maximum growth rates and the unstable frequency range of the disturbances. The molecular weight ratio is a reasonable predictor of the stability trends. We have further demonstrated that the *normalized* growth rate as a function of the convective Mach number is relatively insensitive ($\approx 25\%$) to changes in the composition of the mixing layer. Thus, the *normalized* growth rate is a key element when considering the stability of compressible mixing layers, since once the basic stability characteristics for a particular combination of gases is known at zero Mach number, the decrease in growth rates due to compressibility effects at the larger convective Mach numbers is somewhat predictable.

This work was supported by the National Aeronautics and Space Administration under NASA Contract No. NAS1-19480 while in residence at the Institute for Computer Applications in Science and Engineering (ICASE), NASA Langley Research, Hampton, VA 23681-0001.

1 INTRODUCTION

Inspired by the seminal work of Brown and Roshko[1] and fueled in part by the prospects of high supersonic flight, there since been renewed interest on the stability characteristics of compressible mixing layers, both non-reacting and reacting. All of the analytical investigations of which we are aware have concentrated on mixing layers of a single gas. Experimental investigations have shown that both density ratio and compressibility have a significant effect on the spreading rate of the mixing layer[1, 2, 3]. ¿From experiments it appears that the normalized spreading rate is relatively insensitive to the density ratio as compared to compressibility[3]. However, the density effects have never been analytically quantified. The main thrust of this paper, therefore, is to analyze the stability characteristics of mixing layers in binary gases and to make appropriate comparisons to the case of a single gas.

In investigating the stability of mixing layers, it is typical to assume that there exists a local parallel flow about which the governing equations are linearized with respect to spatially and temporally varying disturbances. From this linearization, it is straightforward to calculate either temporal growth rates (assuming fixed spatial wavenumbers) or to calculate spatial growth rates (assuming a fixed temporal frequency). If a spatial instability exists, there is usually a band or bands of frequencies for which there are positive spatial growth rates (imaginary part of the complex wavenumber is negative). These bands are bounded by the neutral modes, whose existence (and phase speeds) can be determined through the Lees and Lin regularity condition assuming that the phase speeds are subsonic, and that the local flow is smooth and parallel. Another neutral mode can be found in the limit of the wavenumber going to zero. It is clear that in the far downstream limit, the disturbance with the largest spatial growth rate will dominate and thus a disturbance with a single frequency and wavelength (real part of the complex wavenumber) will be seen. However, this scenario neglects non-linear effects which would become significant long before the far downstream limit would be reached. Therefore, it is the entire spectrum of growing modes that is of interest, and the width of the unstable frequency band (and therefore the wavelength band) is significant in determining the structure of the disturbance when nonlinear effects become important.

The results of previous analytical investigations lead to the conclusion that the temperature profile, which is significantly affected by external heating or cooling, internal viscous heating or even exothermic chemical reactions, can alter the regularity condition sufficiently such that an additional pair of unstable modes exist (e.g., the review articles by Jackson[4] and Grosch[5]). In the absence of reaction, viscous heating which is a function of Mach number, significantly raises the temperature so that at a large enough Mach number, there are three neutral modes instead of one. Jackson and Grosch[6] showed that although these additional modes lie in a region in which the phase speeds would typically be supersonic, significant obliqueness of the disturbances alters the sonic phase-speed curves such that all three neutral modes represent a physically realizable subsonic mode. In the case of a reacting mixing layer, a simple $Fuel + Oxidizer \rightarrow Product$ exothermic reaction with moderate heat release easily may introduce an extra pair of neutral modes, even at zero Mach number. A "flame sheet" analysis can be used to quickly locate these

modes, one of which has a phase speed equal to the flow velocity at the flame-sheet location. An extensive study of the spatially evolving reacting mixing layer with finite reaction rate (Hu, et al.[7]) showed that the flame-sheet results gave accurate values of the phase speeds of the neutral modes as long as the Lees and Lin regularity condition was applied downstream of the ignition point. Further analysis showed that the slow mode may undergo a transition from convective to absolute instability as the heat of reaction increases. Although this transition is deemed significant, it was found that the backwards propagation of the disturbance, which is the hallmark of an absolute instability, is seen to be (after a wave packet analysis) exceedingly small.

The purpose of this paper is to investigate the stability characteristics of a mixing layer in a binary gas. In section 2 the the mean flow is discussed. Also given are three models for the viscosity, thermal conductivity, mass species diffusion coefficient and specific heat. These thermodynamic quantities must be defined in some manner before a solution can be obtained. The first two models stated are approximations to the exact third model, in that standard approximations to the viscosity are made in the first two models but not in the third; namely, Chapman's linear viscosity law and Sutherland's viscosity law are employed in the first two models, respectively, while for the third model the thermodynamic properties are given by reference values found in tables, or equivalently, from first-order formulas derived from kinetic theory for a binary mixture. The first two models are provided so that comparisons can be made to the exact, yet computationally intensive, third model. Section 3 contains the stability formulation of a binary gas, and results are presented for both neutral and unstable modes. Conclusions are given in section 4.

2 MEAN FLOW

As mentioned in the Introduction, all previous investigations on the stability of mixing layers, either reacting or non-reacting, have assumed equal molecular weights for the gases above and below the splitter plate. We present here results illustrating how a binary gas mixture affects the stability characteristics. However, since the stability of any flow depends on the structure of the mean flow, we first present below several models for the mean flow.

Consider a binary gas mixture in a compressible mixing layer with zero pressure gradient lying between streams with different speeds and temperatures. The gases included in this study are hydrogen (H_2), helium (He), neon (Ne), nitrogen (N_2), oxygen (O_2) and argon (Ar). The choice of gases was not arbitrary. Papamoschou and Roshko[3] and Hall, Dimotakis and Rosemann[8] used binary combinations of He, N_2 and Ar in their experiments. In addition, hydrogen is the fuel for proposed scramjet engines. As discussed in Kozusko, et al.[9] there are three parameters governing the structure of the mean flow. These are the velocity ratio β_U, defined as the ratio of the velocity in the stream at $-\infty$ to the velocity in the stream at $+\infty$; the temperature ratio β_T, defined in an analogous manner as the velocity ratio; and the molecular weight ratio W dependent on the particular combination of gases chosen, also defined in a similar manner. Here, $\beta_T > 0$ and $\beta_U \in [0, 1)$ so that the gas in the stream at $-\infty$ is always assumed to be

moving slower relative to the gas at $+\infty$. If β_T is less than one, the gas in the slow freestream is relatively cold compared with that in the fast freestream, and if β_T is greater than one it is relatively hot. Note that we have the following two cases depending on the magnitude of W:

- $\underline{W > 1}$ heavier gas resides in the fast freestream at $+\infty$ and the lighter gas in the slow freestream at $-\infty$; or
- $\underline{W < 1}$ lighter gas resides in the fast freestream at $+\infty$ and the heavier gas in the slow freestream at $-\infty$.

For the inert gases Ar and He (typical gases used in experiments), we see that W can vary between 0.1 for the Ar-He case, and 9.9 for the He-Ar case. Throughout this study we will use the convention that the first gas listed resides in the slow freestream at $-\infty$, while the second gas listed resides in the fast freestream at $+\infty$; i.e., the case Ar-He implies that the gas in the slow freestream is argon, while the gas in the fast freestream is helium. The ratio of molecular weights W for the different gases considered in this study are given in Table 1 of Kozusko, et al.[9]

The nondimensional thermodynamic quantities μ, κ, D_{12} and $C_{P,i}$, rendered nondimensional by the respective values μ_∞, κ_∞, $D_{12,\infty}$ and $C_{P,2,\infty}$ in the freestream at $+\infty$, must be defined in some manner before a solution can be obtained. We state here three models, of increasing complexity, that are used in this study. The first two models listed below are approximations to the exact third model, in that standard approximations to the viscosity are made in the first two models but not in the third; namely, Chapman's linear viscosity law and Sutherland's viscosity law are employed in the first two models, respectively, while the third model employs a viscosity law for binary gases. The first two models are provided so that comparisons can be made to the exact, yet computationally intensive, third model.

- Model I: The first model assumes Chapman's viscosity law $\rho\mu =$ constant with $\mu = \rho D_{12} = \kappa = 1$, but allows for different and constant $C_{P,i}$. Owing to the nondimensionalization, $C_{P,2} = 1$, and $C_{P,1}$ is the ratio of the specific heat of the gas at $-\infty$ divided by the specific heat of the gas at $+\infty$. Thus, the mixture specific heat is given by $C_P = C_{P,1}F_1 + F_2$, where F_i is the mass fraction of species i such that in the freestream at $+\infty$ we have $F_1 = 0$ and $F_2 = 1$, while in the freestream at $-\infty$ we have $F_1 = 1$ and $F_2 = 0$. We remark here that the above assumptions lead to $Pr = Le_i^{-1} = C_P$ for the Prandtl and Lewis numbers. These are not constant throughout the mixing layer as is usually assumed. The reason for allowing both the Prandtl number and the Lewis numbers to vary is to take into account different gases and to capture more of the physics presented in Model III below. If C_P is taken to be a constant, then the mean flow would be independent of molecular weight. In this model, the density does not appear explicitly in the mean flow, and its influence is only felt in the stability calculations.
- Model II: The second model assumes that the non-dimensional viscosity is given by Suther-

land's viscosity law

$$\mu = \frac{aT^{3/2}}{b+T}, \qquad a = 1+b, \quad b = 110.4/T_{ref},$$

where T_{ref} is a non-dimensional reference temperature, taken here to be $T_{ref} = 300$. In addition, we take $\rho D_{12} = \kappa = \mu$. As in Model I, we assume constant but different $C_{P,i}$, with $C_{P,2} = 1$. The comments about non-constant Prandtl and Lewis numbers apply to this model as well as to Model I.

- Model III: The last model assumes that all of the thermodynamic properties are given by experimental values found in tables, or equivalently, from first-order formulas derived from kinetic theory for a binary mixture. A complete description is given in Kozusko, et al.[9] We shall refer to this model as the *exact* model.

For Model III, a complete discussion on the structure of the mean flow for various combinations of gases has recently been presented by Kozusko, et al.[9] Expressions for the viscosity, thermal conductivity, specific heat and binary diffusion coefficients of a binary mixture were utilized so that the Prandtl and Lewis numbers vary across the mixing layer. In the cases considered, these two quantities can vary by factors of approximately 3 and 7, respectively, indicating that it is not quantitatively correct to set these quantities to constants, as is usually done. These variations will influence the stability characteristics, as will be shown below.

3 STABILITY

As is standard in linear stability theory, the flow field is perturbed by introducing two-dimensional wave disturbances of the form $e^{i(\alpha x - \omega t)}$ in the velocity, pressure, temperature, density and mass fractions with amplitudes that are functions of the similarity variable η. The similarity variable has been previously defined in Jackson and Grosch [10]. Here, ω is the frequency and α is the streamwise wavenumber of the disturbance. For spatial theory, ω is required to be real and solutions are sought for which α is complex. For temporal theory, α is assumed to be real and solutions are sought for which ω is complex. The amplification rates of the disturbances are then $-\alpha_i$ or ω_i, respectively. Substitution into the inviscid compressible equations for a binary gas and linearizing yields the compressible Rayleigh's equation for the normal velocity perturbation ϕ

$$\left(\frac{\phi'}{\xi}\right)' - \left[\alpha^2 + \frac{1}{U-c}\left(\frac{U'}{\xi}\right)'\right]\phi = 0, \tag{1}$$

where

$$\xi = \frac{1}{\rho^2}\left[1 - M^2(U-c)^2\rho\frac{\gamma_\infty}{\gamma}\right] \tag{2}$$

and

$$\frac{\gamma-1}{\gamma}\rho C_P T = \frac{\gamma_\infty - 1}{\gamma_\infty}. \tag{3}$$

Here, γ is the ratio of specific heats and c is the complex phase speed $c = \omega/\alpha$. Primes indicate differentiation with respect to the similarity variable η. If the molecular weights are taken to be equal and the thermodynamic quantities are assumed constant ($\gamma = \gamma_\infty$, $\rho T = 1$), then (9) reduces to the classical Rayleigh equation for a single component gas[11].

The boundary conditions for ϕ are obtained by considering the limiting form as $\eta \to \pm\infty$. The solutions are of the form

$$\phi \to \exp(\pm\Omega_\pm \eta), \tag{4}$$

where

$$\Omega_+^2 = \alpha^2 \left[1 - M^2(1-c)^2\right], \qquad \Omega_-^2 = \frac{\alpha^2}{\beta_\rho^2}\left[1 - M^2(\beta_U - c)^2 \left(\frac{\beta_\rho}{\beta_\gamma}\right)\right], \tag{5}$$

and

$$\beta_\rho \beta_T W = 1, \qquad \beta_\gamma = \frac{\gamma_{-\infty}}{\gamma_{+\infty}},$$

defines β_ρ and β_γ, respectively. The ratio β_γ for the different gases considered in this study are given in Table 1. Note that if Ω_+^2 is positive, then the disturbances decay exponentially as $\eta \to +\infty$. If, on the other hand, Ω_+^2 is negative, then the disturbances oscillate, indicating that acoustic waves are radiating away from the mixing layer. Similar statements can be made for Ω_-^2. We therefore define $c_\pm$ to be the values of the phase speed for which $\Omega_\pm^2$ vanishes. Thus

$$c_+ = 1 - \frac{1}{M}, \qquad c_- = \beta_U + \frac{1}{M\sqrt{\beta_\rho/\beta_\gamma}}. \tag{6}$$

Note that c_+ is the phase speed of a sonic disturbance in the fast stream and c_- is the phase speed of a sonic disturbance in the slow stream. At

$$M = M_* \equiv \frac{1 + \sqrt{\beta_\gamma/\beta_\rho}}{1 - \beta_U}, \tag{7}$$

$c_\pm$ are equal. A "convective" Mach number can now be defined for a binary gas as

$$M_c = \frac{M}{M_*} \equiv \frac{M(1-\beta_U)}{1 + \sqrt{\beta_\gamma/\beta_\rho}} = \frac{U_\infty - U_{-\infty}}{a_\infty + a_{-\infty}}, \tag{8}$$

where M_* is the Mach number at which the sonic speeds of the two streams are equal. With this definition, all disturbances are supersonic for $M_c > 1$. This definition of the convective Mach number is based on the freestream Mach number in the laboratory frame and is independent of the speed of the large-scale structures and the speed of the most unstable wave. It is interesting to note that the commonly used heuristic definition of the convective Mach number (last term in (8)) is derivable from linear stability analysis[10].

Further understanding of the role of the convective Mach number can be gained by noting $M_c = 1$ implies that $M = M_*$. This is the largest value of the Mach number for which any subsonic instability waves can exist. For larger values of the Mach number there are *only*

supersonic modes which radiate into one or the other stream. The largest value of the convective Mach number for which *only* subsonic modes can exist is given by

$$M_{c_{MIN}} = min(M_+, M_-)/M_*, \tag{9}$$

where M_* is given by (7) and M_+ is the value of the Mach number for which $c_+ = \beta_u$, and M_- is the value for which $c_- = 1$. In the intermediate range $M_{c_{MIN}} < M_c < 1$ both subsonic and supersonic instability waves can exist.

In Figure 4 we plot M_* versus W for the different binary systems. In this figure, the region $0 \leq W \leq 2$ is expanded to better show the differences at the lower values of W. Also shown in this figure as a dashed line is the corresponding value for a single gas (i.e., $W = \beta_\gamma = 1$). The trend is not monotonic due to the variations in the thermodynamic properties, even when two molecular weight ratios are very close to each other. Note that for $W > 1$, M_* is greater than the corresponding value of a single gas, while for $W < 1$, it is smaller. This figure shows that, in general, the value of W is the best indicator for the value of M_*. The overall increase in M_* as W increases indicates that the value of the freestream Mach number above which no subsonic instability waves can exist also increases. Since the value of M_* changes by a factor of five for the cases with large or small weight ratios and this value is used to define the convective Mach number which characterizes the effects of compressibility, it is seen that the proper accounting of the value of M_* for different gas combinations is important.

The nature of the disturbances and the appropriate boundary conditions can now be illustrated by reference to Figure 4, where we plot $c_\pm$ versus M_c for the particular cases of Ar-He (Figure 4a) and He-Ar (Figure 4b), with $\beta_U = 0.5$ and $\beta_T = 1.5$. When referring to this figure, it should be kept in mind that the value of M_* for the two cases varies by a factor of about five so that the scales in terms of the actual Mach number are quite different. The significance of this figure has been discussed previously by Jackson and Grosch [12, 13, 6]. Thus, the key to understanding the stability characteristics of this flow is the understanding of different parameter regions for which various types of instability modes can exist. One can see from Figure 2 that these curves divide the $c_r - M_c$ plane into four regions, where c_r is the real part of c. Also shown as dashed lines are the bounds for c_r; namely, $c_r \in [\beta_U, 1] \equiv [0.5, 1]$. If a disturbance exists with a M_c and c_r in region 1, then Ω_+^2 and Ω_-^2 are both positive, the disturbance is subsonic at both boundaries, and we classify it as a subsonic mode. In region 3, both Ω_+^2 and Ω_-^2 are negative and hence the disturbance is supersonic at both boundaries, and we classify it as a supersonic-supersonic mode. In region 2, Ω_+^2 is positive and Ω_-^2 is negative, the disturbance is subsonic at $+\infty$ and supersonic at $-\infty$, and we classify it as a fast supersonic mode. Finally, in region 4, Ω_+^2 is negative and Ω_-^2 is positive so the disturbance is supersonic at $+\infty$ and subsonic at $-\infty$, and we classify it as a slow supersonic mode.

Note that the above classification scheme only depends upon the values of the mean flow in the freestreams and is independent of the detail form of the mean flow profile. Thus, this classification scheme is valid for all three models used in this study.

To complete the stability problem, the appropriate boundary conditions of either spatial or temporal stability, for either damped or outgoing waves in the fast and slow freestreams are,

respectively,

$$\phi \rightarrow e^{-\Omega_+ \eta} \quad if \quad c_r > c_+, \qquad \phi \rightarrow e^{-i\eta\sqrt{-\Omega_+^2}} \quad if \quad c_r < c_+, \tag{10}$$

$$\phi \rightarrow e^{\Omega_- \eta} \quad if \quad c_r < c_-, \qquad \phi \rightarrow e^{-i\eta\sqrt{-\Omega_-^2}} \quad if \quad c_r > c_-. \tag{11}$$

Finally, the above formulation is also valid for a mixing layer in a channel with a zero streamwise pressure gradient with an appropriate change in the boundary conditions.

3.1 NEUTRAL MODES

To illustrate how a binary gas alters the stability characteristics, we first present below the neutral phase speeds for various combinations of gases.

If a neutral mode exists in region 1 of Figure 4, then the neutral phase speed c_N is given by $c_N = U(\eta_c)$ provided $\alpha \neq 0$. Here, η_c is the zero of the Lees-Lin regularity condition

$$S(\eta) = \left(\rho^2 U'\right)'. \tag{12}$$

The extra factor of ρ is a result of working in the similarity variable instead of the physical variable. The corresponding neutral wavenumber and frequency must be determined numerically. These modes are called regular subsonic neutral modes. If, on the other hand, a neutral mode exists in regions 2, 3 or 4, the Lees-Lin regularity condition can not be used and thus the phase speed of the neutral modes must, in general, be found numerically. These modes are called singular neutral modes.

Typical plots of $S(\eta)$ are shown in Figure 4 for the binary system of argon and helium using Model III with $M = 0$, $\beta_U = 0.5$ and $\beta_T = 1.5$. In each case there is only one zero of S, although the location differs depending upon which gas lies in the fast freestream. In addition, the zeros are not symmetric about the η-axis when changing from the $Ar - He$ system to the $He - Ar$ system. This asymmetry is due to the asymmetries in the velocity and temperature profiles. The difference in location implies that the neutral phase speed c_N in each case will also be different. The location η_c of the zero of S for the different binary systems are given in Table 2, and the corresponding neutral phase speeds given in Table 3.

To better visualize the overall trends, we plot in Figures 4 and 4 the location of the root of $S(\eta)$ and the neutral phase speeds as a function of the molecular weight ratio W, respectively, for Model III (circles). Also shown in these figures are the results for Model I (asterisks) and Model II (triangles). In each figure, the region $0 \leq W \leq 2$ is expanded to better show the differences at the lower values of W. These figures indicate that in general both quantities increase with W, or, equivalently, decrease with increasing β_ρ. The trends are not monotonic due to the variations in the thermodynamic properties, even when two molecular weight ratios are very close to each other. As an example, the case of $H_2 - Ne$ with $W = 10.011$ has a neutral phase speed of $c_N = 0.896$, while the case of $He - Ar$ with $W = 9.979$ has a neutral phase speed of $c_N = 0.919$, which represents an increase in phase speed of 2.5% even though the molecular weight ratio is decreased by only 0.3%. Another example is that of $Ar - Ne$ with $W = 0.505$ and phase speed

of $c_N = 0.735$, and $He - H_2$ with $W = 0.504$ and phase speed of $c_N = 0.780$, which represents an increase of almost 6% in the neutral phase speed even though the molecular weight ratio is decreased by only 0.2%. Qualitatively, the results for all the models are similar, however, there are quantitative differences. For example, neither Models I nor II faithfully reproduce the neutral phase speeds of Model III for the entire range of W considered, although the location η_c for Models II and III are close for $W > 4$. These results indicate that although Models I and II may be simpler to solve numerically than Model III, they do not yield satisfactory agreement over the whole range of W.

In addition to the neutral modes with $\alpha_N \neq 0$, there may exist neutral modes having zero wavenumber. The phase speed of such modes do not satisfy the Lees-Lin regularity condition but are found by an asymptotic analysis of (1) in the limit $\alpha \to 0$ (Grosch, et al. [14]). In this case an expansion of the solution in powers of α, along the lines previously used by Drazin and Howard[15] and Blumen, Drazin and Billings[16] in related studies, yields an eigenvalue relation which is analytically tractable. Below, we shall describe the extension of these results for binary gases.

The leading order term in an α-expansion is independent of the detailed form of the mean profile, and only depends on the basic flow characteristics at infinity. This is to be expected from physical arguments because the wavelength of the instability in the limit $\alpha \to 0$ is much larger than the length scale over which the undisturbed flow is non-uniform. For the supersonic-supersonic case, setting the leading-order term in the expansion to zero yields an equation for c_N:

$$[M^2(\beta_U - c_N)^2\beta_\rho\beta_\gamma^{-1} - 1](1 - c_N)^4 = \beta_\rho^2[M^2(1 - c_N)^2 - 1](\beta_U - c_N)^4. \tag{13}$$

If the molecular weights are taken to be equal and the thermodynamic quantities are assumed constant ($\gamma = \gamma_\infty$, $\rho T = 1$), then equation (13) reduces to equation (5.3a) of Miles [17] expressed in the notation used here. In general, this sixth-order polynomial must be solved numerically to determine c_N as a function of M. For the special case of $\beta_\gamma = 1$, we see that:

[1] A single positive real root of (13) exists for

$$M \geq M_* \equiv (1 + \beta_\rho^{-1/2})/(1 - \beta_U), \tag{14}$$

with phase speed

$$c_N = (\beta_U + \beta_\rho^{-1/2})/(1 + \beta_\rho^{-1/2}). \tag{15}$$

This is classified as a constant speed supersonic-supersonic neutral mode lying in region 3 of the $c_r - M$ plane. It is independent of Mach number and corresponds to the phase speed at which the sonic speeds in the two streams are equal. In this regime there is also a pair of complex conjugate eigenvalues correspond to one unstable and one stable eigenmode. The associated instability disappears as the Mach number increases.

[2] A double root first appears at

$$M_{CR} = (1 + \beta_\rho^{-1/3})^{3/2}/(1 - \beta_U), \tag{16}$$

with phase speed

$$c_N = (\beta_U + \beta_\rho^{-1/3})/(1 + \beta_\rho^{-1/3}). \tag{17}$$

There are three distinct real roots for $M > M_{CR}$. One of these is the phase speed of the constant speed supersonic-supersonic neutral mode while the other two roots must be found numerically from (13). We note that all three of these neutral modes lie in region 3.

3.2 GROWTH RATES

The Rayleigh equation must be solved numerically in order to compute the growth rates. Our experience has shown that it is computationally easier to solve a Riccati type equation, which is a first order, nonlinear, nonhomogenous equation with nonzero boundary conditions, rather then solving a second order, linear, homogeneous equation with zero boundary conditions. To this end, we first begin with the equivalent perturbation equation for the pressure amplitude Π, given by

$$\Pi'' - \frac{2U'}{U-c}\Pi' - \alpha^2 \xi \Pi = 0, \tag{18}$$

which is transformed to an equivalent Riccati equation

$$G' + \alpha T G^2 - \left[\frac{2U'}{U-c} - \frac{T'}{T}\right] G = \frac{\alpha \xi}{T} \tag{19}$$

by use of the transformation

$$G = \frac{\Pi'}{\alpha T \Pi}. \tag{20}$$

Appropriate boundary conditions can be derived in a straightforward manner. Further details can be found in Jackson and Grosch [10]. The stability problem is thus to solve the Riccati equation, together with appropriate boundary conditions, for a given real frequency ω and Mach number M, with the mean profile defined for a particular binary gas. The eigenvalue is the wavenumber α. We integrate the Riccati equation along the contour $\eta = -L$ to $\eta = 0$ and $\eta = L$ to $\eta = 0$ using a fourth-order Runge-Kutta scheme. The value of L varied from mixture to mixture, and was chosen large enough so that in each case the boundary conditions were satisfied. We choose an initial α and then iterate using Muller's method[18], until the boundary conditions were satisfied and the differences in all calculated quantities at $\eta = 0$ was less than 10^{-6}. All calculations were done in 64 bit precision. Because this equation has a singularity at $U = c_N$, the neutral modes could not be determined.

The spatial growth rates for selected binary mixtures as a function of frequency are shown in Figures 4-4 for Models I, II and III, respectively. In all cases, $M = 0$, $\beta_U = 0.5$ and $\beta_T = 1.5$. In each figure, the labeled curves correspond to binary gases with increasing molecular weight ratio W. ¿From these figures several remarks can be made. For a given model, there is a general decrease in the maximum growth rate as the molecular weight ratio increases. This is consistent with the limited experimental evidence that the growth rate is smaller when the heavier gas is on the high-speed side and greater when the heavier gas is on the the low-speed side[3]; as we shall see below, this statement is not strictly true for all of the gas combinations studied here. The

largest growth rate for Model I (which corresponds to the smallest value of W shown in Figure 4) is more than twice the largest growth rate shown for the other two models. As the value of W increases, the maximum growth rate decreases to the point where the numerical error, due to the presence of the critical layer, is of the same order as the growth rates, and thus the procedure can not be continued for the largest values of W (e.g., see the curve labeled 7 in Figure 4). Note also that the largest range of frequency shown in Model I is more than three times larger than the frequency ranges shown for the other two models. This is particularly significant since Model I would imply a much larger range of unstable wavelengths than is actually present. The range of unstable wavelengths could ultimately determine the turbulent structures that might develop. Of further note, is the differences in the neutral phase speeds as seen in Figure 4 which are predictive of the real phase speeds of the unstable wave packet.

A more direct comparison of the maximum growth rates between the three models for a given binary system can be found in Table 4. Here, the maximum growth rates for twenty-four combinations are listed. The maximum growth rate for a single species gas using Sutherland's viscosity law with $Pr = 0.7$ is $\alpha_{i,max} = -0.047541$. Note that the maximum growth rates for any of the three models is not a strictly decreasing function of W. There is some variation of the general rule when specific combinations of gases are used owing to the difference in the actual physical parameters. Also shown in the table are the relative errors between Models I and II with Model III. From this table one can see that Model I over predicts the maximum growth rates of Model III considerably for small values of W (the first nine binary gases listed) and under predicts for large values of W (the last four or six binary gases listed). This trend is observed for Model II, but is less severe than for Model I.

The above results indicate that the stability results for Models I and II are a poor approximation to the stability results for Model III.

The spatial growth rates for various values of the convective Mach number M_c, as defined by (8), are shown in Figure 4 for Model III for the gases nitrogen and argon. In all cases, $\beta_U = 0.5$ and $\beta_T = 1.5$. In each case, the maximum growth rate, the corresponding frequency at which the maximum is attained, and the range of frequencies over the entire unstable spectrum decreases as the convective Mach number increases. Once the growth-rate *vs* frequency curve is found for $M_c = 0$, the $M_c > 0$ curves appear to be nested in a predictable manner. To further explore this, consider the normalized growth rate, defined as

$$R = \frac{-\alpha_{i,max}(M_c)}{-\alpha_{i,max}(0)}. \tag{21}$$

The normalized growth rates for the gas combinations Ar-N_2 (circle), N_2-Ar (plus), N_2-He (diamond) and O_2-H_2 (bullet) are shown in Figure 4. Also shown (solid curve) in this figure is the corresponding results for a single gas using Sutherland's viscosity law with $Pr = 0.7$. We note here that for the cases of Ar-N_2 and N_2-Ar, both the Lewis number and the Prandtl number are nearly constant across the shear layer (see figures 1 and 4 of Kozusko, et al.[9]). For the case of N_2-He the Lewis number varies by a factor of 8 across the mixing layer (see figure 3 of Kozusko, et al.[9]) while the Prandtl number varies considerably (see figure 6 of Kozusko, et

al.[9]). Finally, for the case of O_2-H_2 the Lewis number varies by a factor of 6 across the mixing layer (see figure 2 of Kozusko, et al.[9]) while the Prandtl number again varies considerably (see figure 5 of Kozusko, et al.[9]). At $M_c = 1.0$, there is a spread in the normalized growth rates between the various gas combinations of about 25%. The consistent shape of the curves in Figure 4 indicate that there is almost a similarity-like behavior when determining the decrease in the growth rate owing to an increase in convective Mach number. Indeed, other gas combinations produce similar results. This is consistent with the results of Jackson and Grosch[10] where it was determined that for a single gas ($\beta_\gamma = 1$) with $M_c < 1$, the actual mean flow velocity and temperature profiles did not matter when determining the normalized growth rate as a function of the convective Mach number. Thus, as previously suspected, this analysis shows that the decrease in growth rates with increasing Mach number is due to compressibility effects and is only somewhat modified by considering specific combinations of gases (and thus varying the density ratios). Knowing the maximum growth rate at $M_c = 0$, one could easily estimate an approximate value of the growth rate when $M_c \neq 0$ using a single gas and any of the various models for the mean flow (*i.e.*, Chapman's Law, Sutherland's Law, or even a hyperbolic tangent profile). However, we have shown that the maximum growth rates (and corresponding frequency ranges and wavelength ranges) differ substantially at $M_c = 0$ and that the simplified models (Model I and Model II) are poor predictors of these values.

4 CONCLUSION

The two-dimensional inviscid spatial stability characteristics of a compressible mixing layer with a binary combination of gases is presented. ¿From the analysis above, we conclude that differing molecular weights has a significant effect on the neutral-mode phase speeds, the phase speeds of the unstable modes, the maximum growth rates and the unstable frequency range of the disturbances. The molecular weight ratio is a reasonable (if not perfect) predictor of the trends. It was also determined that the various models that have been previously used are valid in predicting the general trends, but are poor choices if quantitative information is needed. We have further demonstrated that the relative insensitivity ($\approx 25\%$) of the *normalized* growth rate as a function of the convective Mach number is a key element when considering compressible mixing layers. Once the basic stability characteristics for a particular combination of gases is known at zero Mach number, the decrease in growth rates due to compressibility effects at the larger convective Mach numbers is predictable.

References

[1] G.L. Brown and A. Roshko, "On density effects and large structure in turbulent mixing layers", J. Fluid Mech. **64**, 775 (1974).

[2] D.W. Bogdanoff. "Interferometric measurement of heterogeneous shear-layer spreading rates", AIAA J. **22**, 1550 (1984).

[3] D. Papamoschou and A. Roshko, "The compressible turbulent shear layer: An experimental study", J. Fluid Mech. **197**, 453 (1988).

[4] T.L. Jackson, "Stability of laminar diffusion flames in laminar mixing layers," in *Major Research Topics in Combustion*, edited by M.Y. Hussaini, A. Kumar, and R.G. Voigt (Springer, New York, 1992), p. 131.

[5] C.E. Grosch, "Reacting compressible mixing layers:structure and stability", in *Combustion in High-Speed Flows*, edited by J. Buckmaster, T.L. Jackson, and A. Kumar (Kluwer, 1994), p. 131.

[6] T.L. Jackson and C.E. Grosch, "Inviscid spatial stability of a compressible mixing layer. Part iii. Effect of thermodynamics", J. Fluid Mech. **224**, 159 (1991).

[7] F.Q. Hu, T.L. Jackson, D.G. Lasseigne, and C.E. Grosch, "Absolute/convective instabilities and their associated wave packets in a compressible mixing layer", Phys. Fluids A **5**, 901 (1993).

[8] J.L. Hall, P.E. Dimotakis, and H. Rosemann, "Experiments in non-reacting compressible shear layers study", AIAA Paper 91-0629 (1991).

[9] F. Kozusko, C.E. Grosch, T.L. Jackson, T.B. Gatski, and C.A. Kennedy, "The structure of variable property, compressible mixing layers in binary gas mixtures", Phys. Fluids, submitted (1995).

[10] T.L. Jackson and C.E. Grosch, "Absolute/convective instabilities and the convective Mach number in a compressible mixing layer", Phys. Fluids A **6**, 949 (1990).

[11] P.G. Drazin and W.H. Reid, *Hydrodynamic stability* (Cambridge University Press, 1984).

[12] T.L. Jackson and C.E. Grosch, "Inviscid spatial stability of a compressible mixing layer", J. Fluid Mech. **208**, 609 (1989).

[13] T.L. Jackson and C.E. Grosch, "Inviscid spatial stability of a compressible mixing layer. Part ii. The flame sheet model", J. Fluid Mech. **217**, 391 (1990).

[14] C.E. Grosch, T.L. Jackson, R. Klein, A. Majda, and D.T. Papageorgiou, "The inviscid discrete eigenvalue spectrum of the compressible mixing layer", (unpublished manuscript). A detailed discussion appears in the review article by Grosch[3], 1991.

[15] P.G. Drazin and L.N. Howard, "The instability to long waves of unbounded parallel flow", J. Fluid Mech. **14**, 257 (1962).

[16] P.G. Drazin W. Blumen and D.F. Billings, "Shear layer instability of an inviscid compressible fluid. Part 2", J. Fluid Mech. **71**, 305 (1975).

[17] J.W. Miles, "On the disturbed motion of a plane vortex sheet", J. Fluid Mech. **4**, 538 (1958).

[18] W.H. Press, S.A. Teukolsky, W.T. Vetterling and B.P. Flannery, *Numerical Recipes in Fortran* (Cambridge University Press, 1992).

Table 1: The ratio β_γ, defined as the ratio of specific heats at $\eta = -\infty$ divided by the ratio of specific heats at $\eta = +\infty$, for the different gases considered in this study. The top row corresponds to the gases in the freestream at $\eta = +\infty$, while the first column corresponds to the gases in the freestream at $\eta = -\infty$.

	H_2	He	Ne	N_2	O_2	Ar
H_2	0.995	0.839	0.839	0.999	1.002	0.839
He	1.186	1.000	1.000	1.191	1.195	1.000
Ne	1.186	1.000	1.000	1.191	1.195	1.000
N_2	0.992	0.836	0.836	0.996	1.000	0.836
O_2	0.977	0.824	0.824	0.981	0.985	0.824
Ar	1.186	1.000	1.000	1.191	1.195	1.000

Table 2: The location $S(\eta_c) = 0$, as determined from Model III, at $M = 0$, $\beta_U = 0.5$ and $\beta_T = 1.5$ for the different gases considered in this study. The top row corresponds to the gases in the freestream at $\eta = +\infty$, while the first column corresponds to the gases in the freestream at $\eta = -\infty$. The notation NA means not applicable for a binary gas.

	H_2	He	Ne	N_2	O_2	Ar
H_2	NA	0.096	0.124	0.228	0.208	0.186
He	0.219	NA	0.246	0.373	0.346	0.317
Ne	-0.313	-0.255	NA	0.379	0.364	0.368
N_2	-0.795	-0.583	-0.057	NA	0.168	0.178
O_2	-0.814	-0.617	-0.052	0.200	NA	0.200
Ar	-1.013	-0.769	-0.110	0.153	0.145	NA

Table 3: The corresponding neutral phase speeds c_N, as determined from Model III, at $M = 0$, $\beta_U = 0.5$ and $\beta_T = 1.5$ for the different gases considered in this study. The top row corresponds to the gases in the freestream at $\eta = +\infty$, while the first column corresponds to the gases in the freestream at $\eta = -\infty$. The notation NA means not applicable for a binary gas.

	H_2	He	Ne	N_2	O_2	Ar
H_2	NA	0.829	0.896	0.922	0.924	0.926
He	0.780	NA	0.892	0.914	0.916	0.919
Ne	0.668	0.690	NA	0.851	0.856	0.868
N_2	0.628	0.649	0.757	NA	0.817	0.829
O_2	0.627	0.646	0.753	0.808	NA	0.826
Ar	0.614	0.631	0.735	0.789	0.794	NA

Table 4: The maximum spatial growth rates for various binary systems and for the three models used in the study. The gases are listed in increasing W. Also shown are the relative errors between Models I and II with Model III. The relative error is defined as the maximum growth rate of Model III minus the maximum growth rate of Model I or II, divided by the maximum growth rate of Model III. NA implies not available. Here, $M = 0$, $\beta_U = 0.5$ and $\beta_T = 1.5$.

F_1	F_2	Model I	Model II	Model III	ERR(I,III)%	ERR(II,III)%
Ar	H_2	-0.2672	-0.0558	-0.0652	-309	14
O_2	H_2	-0.2332	-0.0562	-0.0670	-248	16
N_2	H_2	-0.2317	-0.0587	-0.0704	-229	16
Ar	He	-0.2225	-0.0697	-0.0818	-172	14
Ne	H_2	-0.1448	-0.0593	-0.0619	-133	4
O_2	He	-0.1876	-0.0687	-0.0809	-131	15
N_2	He	-0.1799	-0.0697	-0.0846	-112	17
Ne	He	-0.1229	-0.0676	-0.0700	-75	3
He	H_2	-0.0744	-0.0612	-0.0550	-35	-11
Ar	Ne	-0.0754	-0.0599	-0.0709	-6	15
O_2	Ne	-0.0626	-0.0540	-0.0647	3	16
Ar	N_2	-0.0626	-0.0561	-0.0557	-12	0
N_2	Ne	-0.0578	-0.0519	-0.0652	11	20
Ar	O_2	-0.0521	-0.0538	-0.0550	5	2
O_2	N_2	-0.0521	-0.0498	-0.0500	-4	0
N_2	O_2	-0.0437	-0.0448	-0.0486	10	7
O_2	Ar	-0.0390	-0.0409	-0.0437	10	6
Ne	N_2	-0.0396	-0.0430	-0.0395	0	-8
N_2	Ar	-0.0355	-0.0385	-0.0430	17	10
Ne	O_2	-0.0357	-0.0403	-0.0381	6	-5
Ne	Ar	-0.0279	-0.0337	-0.0333	16	-1
H_2	He	-0.0274	-0.0321	-0.0434	36	26
He	Ne	-0.0100	-0.0173	-0.0238	57	27
He	N_2	NA	-0.0140	-0.0178	NA	21

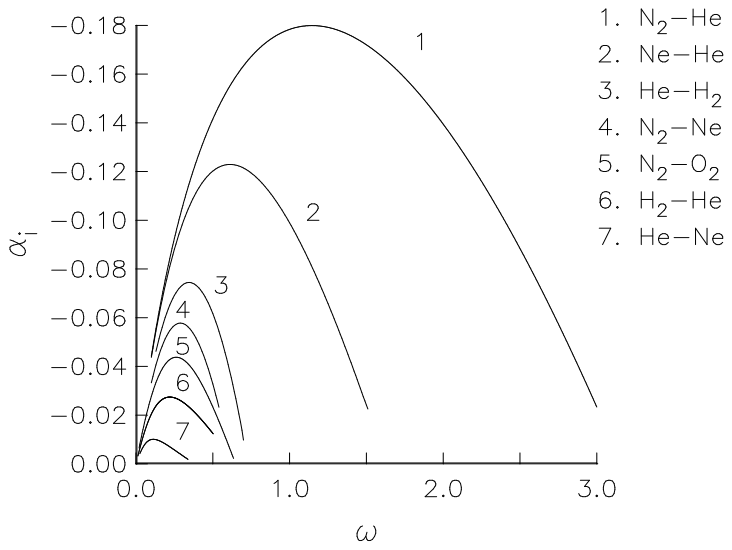

Figure 1: Plot of M_* versus W for the different binary systems. Also shown in this figure as a dashed line is the corresponding value for a single gas (i.e., $W = \beta_\gamma = 1$). Here, $\beta_U = 0.5$ and $\beta_T = 1.5$.

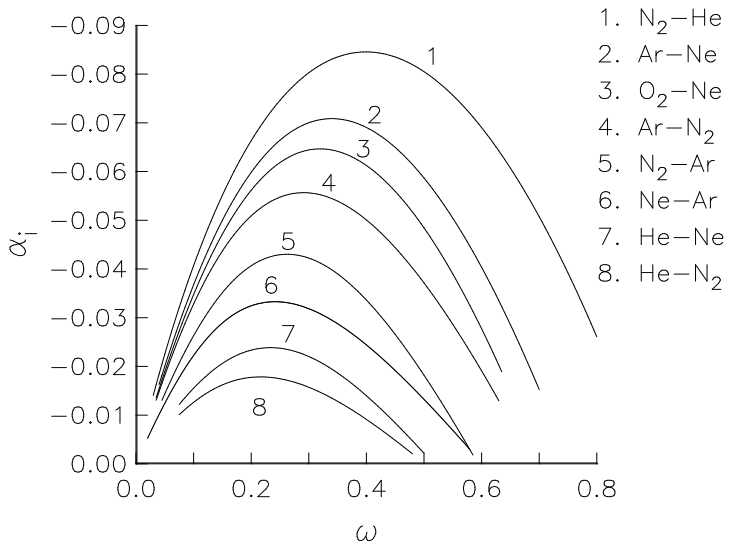

Figure 2: Plot of $c_{\pm}$ versus M_c for the particular cases of (a) Ar-He and (b) He-Ar, with $\beta_U = 0.5$ and $\beta_T = 1.5$. These curves divide the $c_r - M_c$ plane into four regions: (1) subsonic; (2) fast supersonic; (3) supersonic-supersonic; and (iv) slow supersonic.

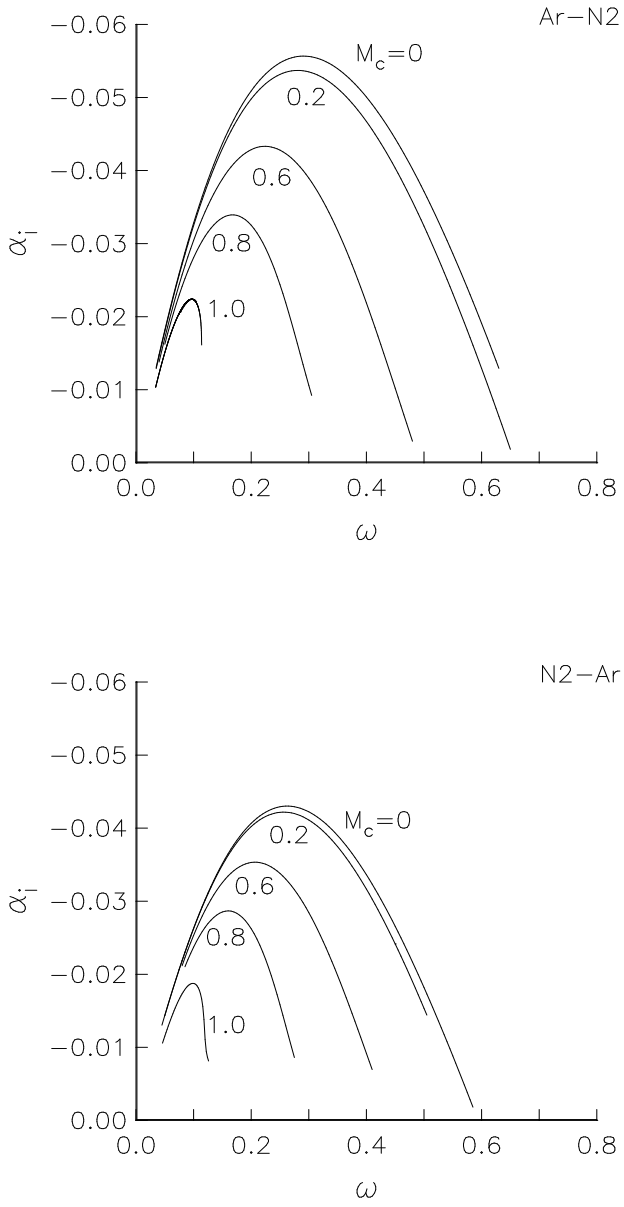

Figure 3: Plot of $S(\eta)$ for (a) Ar-He and (b) He-Ar using Model III with $M = 0$, $\beta_U = 0.5$ and $\beta_T = 1.5$.

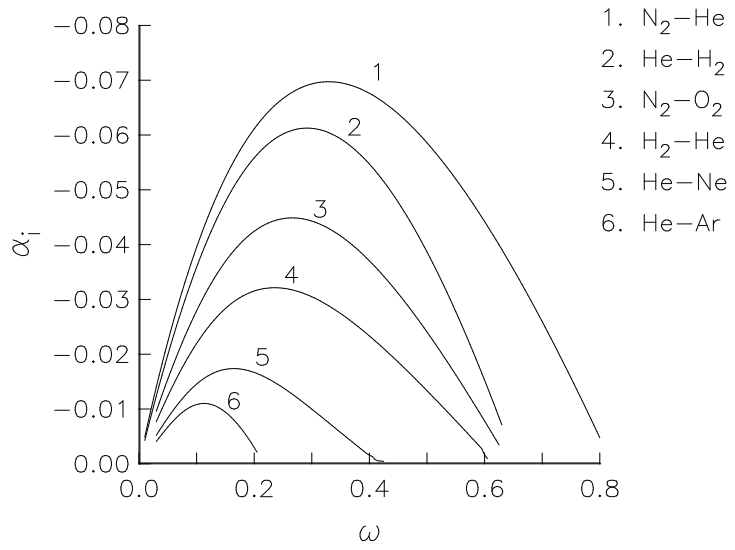

Figure 4: Plot of the location η_c as a function of the molecular weight ratio W using Model I (asterisks), Model II (triangles), and Model III (circles) with $M = 0$, $\beta_U = 0.5$ and $\beta_T = 1.5$.

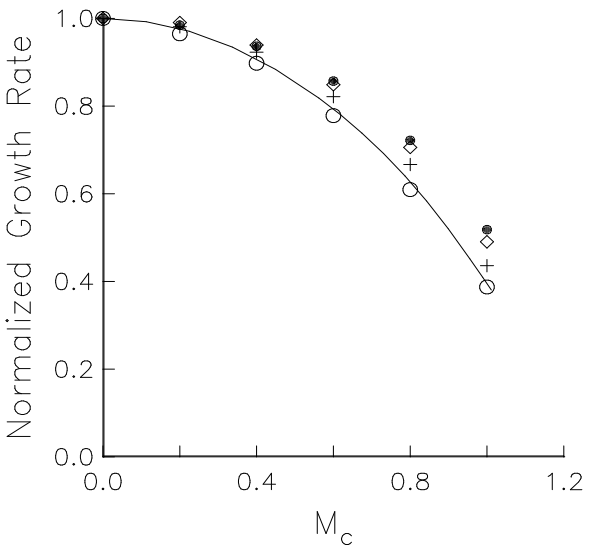

Figure 5: Plot of the neutral phase speeds c_N as a function of the molecular weight ratio W using Model I (asterisks), Model II (triangles), and Model III (circles) with $M = 0$, $\beta_U = 0.5$ and $\beta_T = 1.5$.

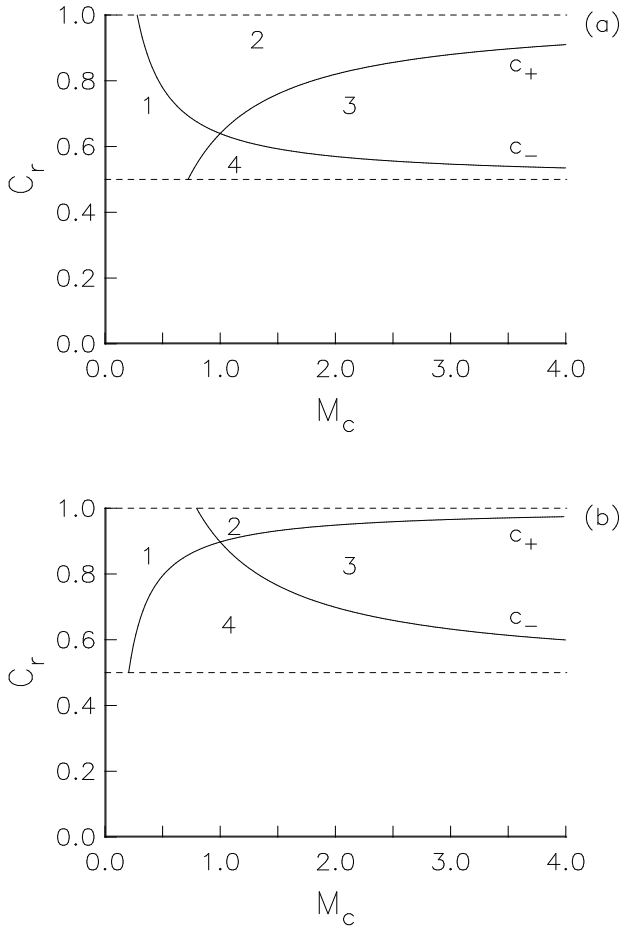

Figure 6: The spatial growth rates for selected binary mixtures as a function of frequency for Model I with $M = 0$, $\beta_U = 0.5$ and $\beta_T = 1.5$. In each figure, the labeled curves correspond to binary gases with increasing molecular weight ratio W, with 1 being the combination with the smallest value of W.

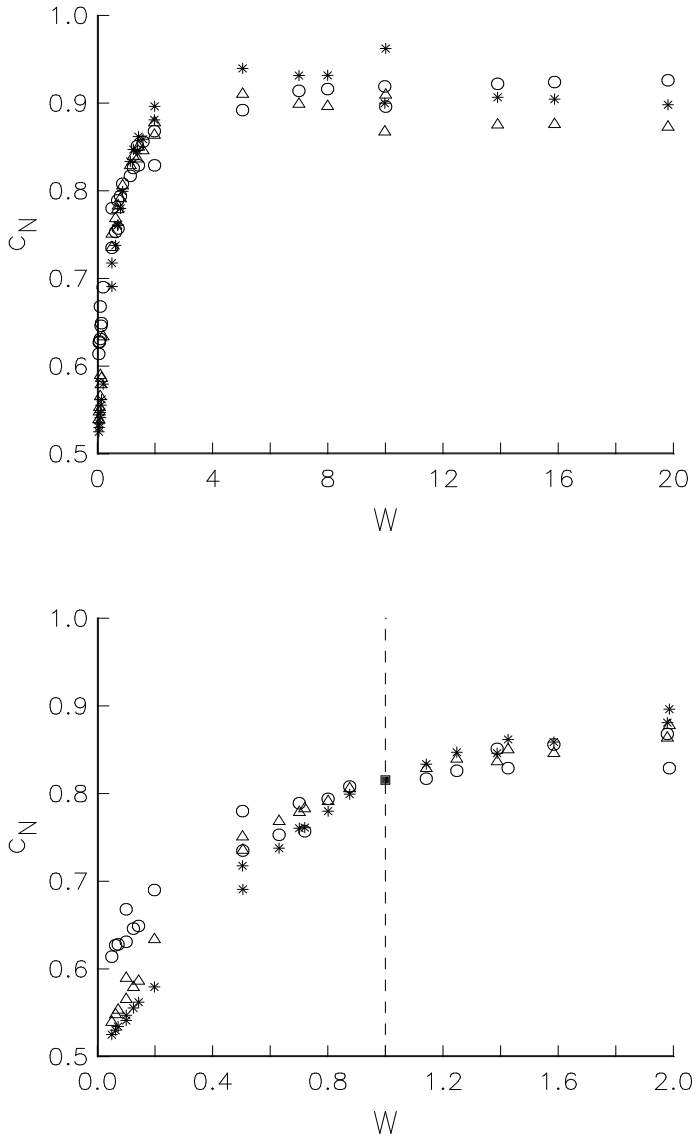

Figure 7: The spatial growth rates for selected binary mixtures as a function of frequency for Model II with $M = 0$, $\beta_U = 0.5$ and $\beta_T = 1.5$. In each figure, the labeled curves correspond to binary gases with increasing molecular weight ratio W, with 1 being the combination with the smallest value of W.

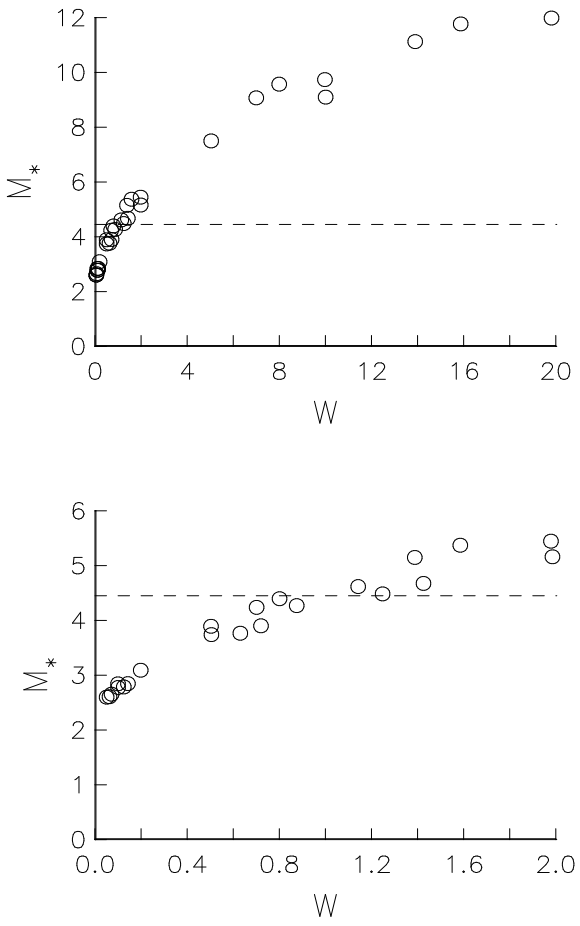

Figure 8: The spatial growth rates for selected binary mixtures as a function of frequency for Model III with $M = 0$, $\beta_U = 0.5$ and $\beta_T = 1.5$. In each figure, the labeled curves correspond to binary gases with increasing molecular weight ratio W, with 1 being the combination with the smallest value of W.

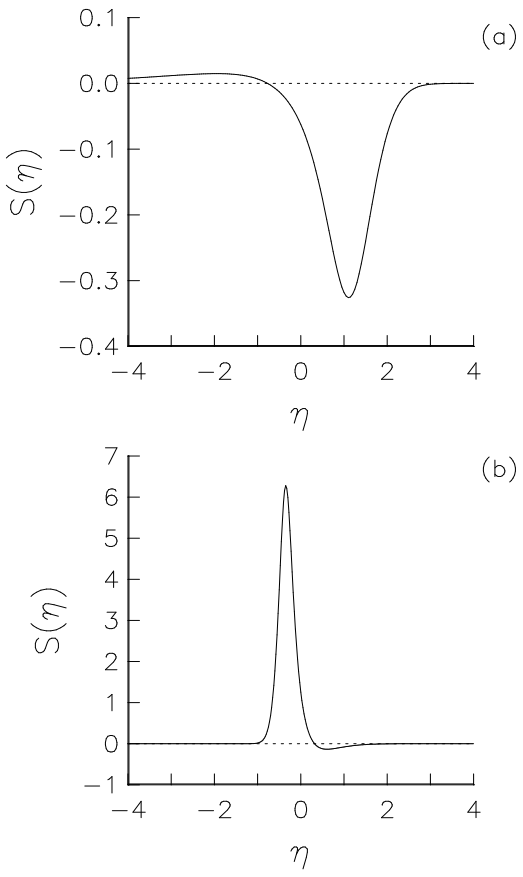

Figure 9: Plot of the spatial growth rates for various values of the convective Mach number M_c, as defined by (8), using Model III for (a) Ar-N_2 and (b) N_2-Ar. Here, $\beta_U = 0.5$ and $\beta_T = 1.5$.

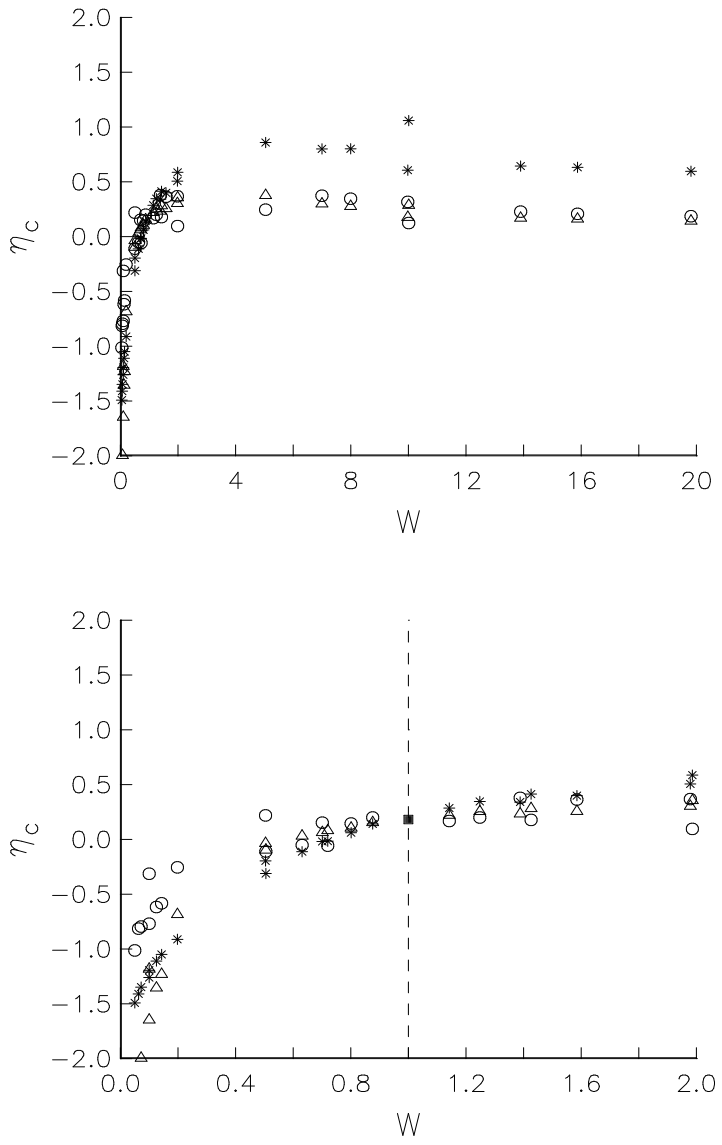

Figure 10: Plot of the normalized growth rate versus the convective Mach number for the binary system Ar-N_2 (circle), N_2-Ar (plus), N_2-He (diamond) and O_2-H_2 (bullet) using Model III with $\beta_U = 0.5$ and $\beta_T = 1.5$. The solid curve corresponds to the results for a single species gas.